



Molecular Crystals and Liquid Crystals

Publication details, including instructions for authors and subscription information:

<http://www.tandfonline.com/loi/gmcl20>

Some Properties of Nematic Liquid Crystal E7/Acrylic Polymer Networks

Y. Derouiche^{a b c}, F. Dubois^b, R. Douali^b, C. Legrand^b & U. Maschke^a

^a Unité Matériaux et Transformations (UMET), Université de Lille - Sciences et Technologies, Villeneuve d'Ascq Cedex, France

^b UDSMM-LEMCEL, Université du Littoral - Côte d'Opale, Calais, France

^c Département des Sciences de la Matière, Faculté des Sciences et Technologies, Université ZIANE Achour de Djelfa, Cité juillet Djelfa, Calais, Algérie

Version of record first published: 30 Jun 2011

To cite this article: Y. Derouiche, F. Dubois, R. Douali, C. Legrand & U. Maschke (2011): Some Properties of Nematic Liquid Crystal E7/Acrylic Polymer Networks, *Molecular Crystals and Liquid Crystals*, 541:1, 201/[439]-210/[448]

To link to this article: <http://dx.doi.org/10.1080/15421406.2011.569231>

PLEASE SCROLL DOWN FOR ARTICLE

Full terms and conditions of use: <http://www.tandfonline.com/page/terms-and-conditions>

This article may be used for research, teaching, and private study purposes. Any substantial or systematic reproduction, redistribution, reselling, loan, sub-licensing, systematic supply, or distribution in any form to anyone is expressly forbidden.

The publisher does not give any warranty express or implied or make any representation that the contents will be complete or accurate or up to date. The accuracy of any instructions, formulae, and drug doses should be independently verified with primary sources. The publisher shall not be liable for any loss, actions, claims, proceedings, demand, or costs or damages whatsoever or howsoever caused arising directly or indirectly in connection with or arising out of the use of this material.

Some Properties of Nematic Liquid Crystal E7/Acrylic Polymer Networks

Y. DEROUCHE,^{1,2,3} F. DUBOIS,² R. DOUALI,²
C. LEGRAND,² AND U. MASCHKE¹

¹Unité Matériaux et Transformations (UMET), Université de Lille –
Sciences et Technologies, Villeneuve d'Ascq Cedex, France

²UDSMM-LEMCEL, Université du Littoral – Côte d'Opale,
Calais, France

³Département des Sciences de la Matière, Faculté des Sciences et
Technologies, Université ZIANE Achour de Djelfa, Cité juillet Djelfa,
Calais, Algérie

Polymer Dispersed Liquid Crystal films were elaborated by photopolymerization using ultraviolet radiation of liquid crystal/monomer mixtures. Three acrylic difunctional propyleneglycol based monomers were used; differing only by their chain lengths in terms of their molecular weight. Infrared spectroscopy investigation made it possible to obtain the monomer conversion rates, in order to determine the effect of the presence of liquid crystal on the kinetics of polymerization and phase separation. The characterization by linear dielectric spectroscopy of the monomers and polymers was carried out as a function of temperature in the frequency range from 20 Hz to 1 MHz.

Keywords Dielectric spectroscopy; differential scanning calorimetry; infrared spectroscopy; liquid crystal; polymer

1. Introduction

Polymer/liquid crystal systems are the subject of intensive investigations in many laboratories around the world [1,2]. This interest is motivated by their potential use in many fields of high technology involving electronic equipments, display systems, commutable windows, etc [1,2]. In particular, PDLC (Polymer Dispersed Liquid Crystal) systems are multicomponent mixtures and can be switched electrically from a light scattering 'OFF' state to a highly transparent 'ON' state. In this work we are particularly interested in an experimental study of the effect of molecular weight of starting materials (monomers) on the thermo-physical and dielectric properties of elaborated polymer/LC systems. Difunctional acrylic propyleneglycol based monomers having similar chemical structures and nematic LC E7 were used.

Address correspondence to U. Maschke, Unité Matériaux et Transformations (UMET), UMR 8207 – CNRS, Université de Lille 1 – Sciences et Technologies, Bâtiment C6, 59655 Villeneuve d'Ascq Cedex, France. Tel.: 0033 3 20 33 63 81; Fax: 0033 3 20 43 43 45; E-mail: ulrich.maschke@univ-lille1.fr

Propyleneglycol diacrylate is a difunctional acrylate monomer that is particularly useful in inkjets and coatings where improved thermal stability is desired under operating conditions. In addition, some components made of propyleneglycol diacrylate exhibit good flexibility, adhesion and moisture resistance, and improved filtration characteristics, which can shorten manufacturing time, and reduce usage of filtration media. The propyleneglycol diacrylate monomers employed in this study are distinguished by their molecular weight between the two reactive chain ends, giving the formation of polymer networks with varying distances between two adjacent crosslinking points. A dielectric study of these three monomers was performed using an impedance bench measurement covering a wide frequency range from 20 Hz to 1 MHz. The aim is to compare the dielectric and thermo-physical properties of the monomers, the corresponding polymer, and selected polymer/LC systems.

2. Materials and Experimental Methods

2.1. Materials

Three acrylic difunctional propyleneglycol based monomers possessing the same chemical structures were used in this study; differing only by their chain lengths in terms of their molecular weight: Tripropyleneglycoldiacrylate (TPGDA) with 300 g/mol, polypropylene-glycoldiacrylate with 540 g/mol (PPGDA540), and polypropyleneglycoldiacrylate with 900 g/mol (PPGDA900).

Samples were prepared from mixtures of X weight-percent (wt.-%) LC and (100-X) wt.-% of the monomer. 2 wt.-% (compared to the acrylate) of 2-hydroxy-2-methyl-1-phenyl-propane-1-one (Darocur 1173) was added as photoinitiator to the initial mixtures before exposure to UV light. All products were used as received.

The nematic LC used in this work is the eutectic mixture E7 (Merck KGaA, Darmstadt, Germany) containing four cyanoparaphenylene derivatives. E7 is made of 51 weight-percent (wt.-%) 4-cyano-4'-pentylbiphenyl (5CB), 25 wt.-% 4-cyano-4'-heptyl-biphenyl (7CB), 16 wt.-% 4-cyano-4'-octyloxybiphenyl (8OCB), and 8 wt.-% 4-cyano-4''-pentyl-p-terphenyl (5CT). This LC mixture exhibits a nematic-isotropic transition temperature at $T_{NI}=61^{\circ}\text{C}$ and a positive dielectric anisotropy $\Delta\epsilon = \epsilon_{//} - \epsilon_{\perp}$ at $T=20^{\circ}\text{C}$, where $\epsilon_{//}$ and ϵ_{\perp} represent the parallel and perpendicular dielectric constants, respectively. The refractive indices of E7 at $T=20^{\circ}\text{C}$ are given as $n_0 = 1.5183$; $n_e = 1.7378$ ($\lambda = 632.8\text{ nm}$) [3,4], leading to a birefringence of $\Delta n = n_e - n_0 = 0.2195$. The chemical structures of the compounds are given in Figure 1.

Each mixture was prepared in duplicate and stirred at room temperature during several hours. Samples for infrared spectroscopy measurements were prepared by sandwiching the initial reactive mixture between a NaCl plate (Sigma Aldrich) and a Polyethylene-terephthalate (PET) sheet (Renker, Germany), allowing a uniform penetration of the applied dose in the depth of the sample. The PET sheet was coated with a thin transparent layer of conducting indium/tin oxide (ITO). This technique avoids undesired oxygen – inhibition effects and is routinely used in our laboratories to prepare polymer/LC materials for different applications.

2.2. Experimental Methods

2.2.1. Differential Scanning Calorimetry (DSC). The Differential Scanning Calorimetry (DSC) was used for the study of polymer/LC composites [5–13] and detection of phase transitions for molecules of low molecular weight such as

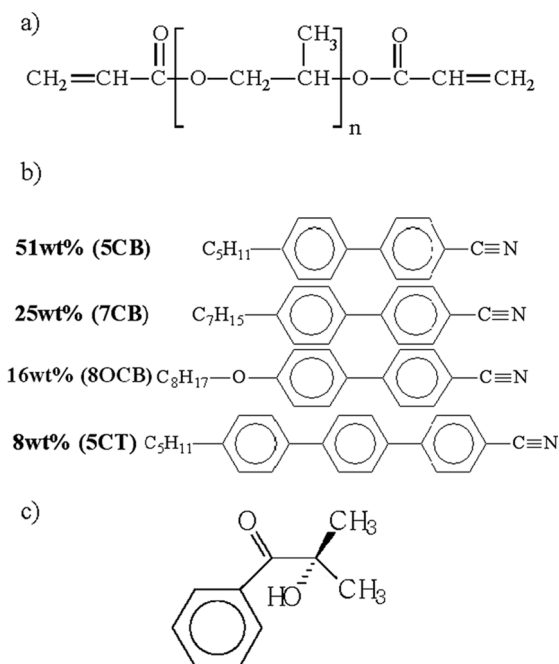


Figure 1. Chemical structures of (a) Polypropyleneglycoldiacrylate PPGDA, (b) the nematic LC mixture E7, (c) the photoinitiator 2-hydroxy-2-methyl-1-phenyl-propane-1-one (Darocur 1173).

the nematic LC E7. DSC measurements were performed on a Perkin Elmer Pyris Diamond calorimeter equipped with an Intracooler 2P system allowing cooling experiments. Samples for calorimetric measurements were prepared by introducing approximately 8 mg of the film into aluminum DSC pans, which have been sealed to avoid evaporation effects during the temperature treatment. A rate of 10°C/min (heating and cooling) was used in the temperature range from -70 to $+100^\circ\text{C}$. The program consists first in cooling the sample followed by three heating and cooling cycles to take into account eventual thermal events related to the sample preparation history. The thermograms presented in this work were obtained from the first heating ramps. In each case, at least three duplicate samples having the same composition and prepared independently were used to check the reproducibility of results. The polymer glass transition temperature was determined from the midpoint of the transition range of the thermograms.

2.2.2. Infrared Spectroscopy. FTIR spectra of thin films (less than $10\mu\text{m}$) in the transmission mode were recorded at room temperature with a Perkin Elmer 2000 model before and after UV exposure. Each dose was applied once and the interval of time between the end of exposure and the infrared analysis was kept constant (below one minute). The number of accumulated scans was 16 with a spectral resolution of 4cm^{-1} . The experiments were repeated three times to validate the results and check if they are reproducible.

2.2.3. Dielectric Spectroscopy. The dielectric characterization set-up is made of an HP4284A impedance analyser, and a measuring cell which allows performing

measurements in a frequency range 20 Hz–1 MHz. The measuring ac voltage is fixed to 0.1 V_{rms}. The real $\varepsilon'(f)$ and imaginary $\varepsilon''(f)$ parts of the complex permittivity ε^* ($\varepsilon^*(f) = \varepsilon'(f) - j\varepsilon''(f)$) are calculated from the measured capacitance C and conductance G:

$$\varepsilon'(f) = \frac{C(f)}{C_0} \quad (1)$$

$$\varepsilon''(f) = \frac{G(f)}{2\pi f C_0} \quad (2)$$

where C_0 is the empty cell capacitance measured before cell filling. The temperature was stabilized with a temperature controller (Oxford Instrument ITC601 with platinum sensor) with a accuracy better than 0.1°C; the experimental set-up is controlled via a PC computer equipped with HPVEE software.

The measuring cell of dielectric spectroscopy consists of a planar capacitor made of two glass plates [14]. To obtain an electrical contact, the first plate is covered by gold and the second one by ITO which is transparent and allows thus to check the filling of the cell. The sample thickness of 25 μm was fixed with mica or double-sided self-adhesive tape spacers. The electrical contact on the electrodes is made with coaxial connectors (SMA standard). The sample is introduced by capillarity. For the LC, the dielectric characterization is usually carried out using oriented LC molecules. Since, the total orientation of LC molecules vanishes, and no orientation layers were used for polymer/LC materials.

3. Results and Discussion

3.1. Differential Scanning Calorimetry (DSC)

Figure 2 shows selected regions of DSC thermograms for the three polymer/LC systems: 30 wt% TPGDA/70 wt% E7, 30 wt% PPGDA540/70 wt% E7, 30 wt% PPGDA900/70 wt% E7, and pure E7. In the temperature range chosen for this study (−70°C to 100°C), two characteristic transitions were detected for each system studied: on the left hand side of Figure 2, the glass transition of the LC domains dispersed in the polymer matrix (T_g (E7)); and on the right hand side, the nematic-isotropic transition (T_{NI}) of these segregated LC domains at higher temperatures. In Table 1 are summarized the values of T_g (polymer matrix), T_g (E7) and T_{NI} , obtained for the different samples investigated.

The glass transition temperature of LC confined in the polymer matrix remains almost constant with a slight variation of approximately 1°C for the three polymer/LC systems, compared to pure E7. The results from Figure 2 (see also Table 1) show clearly the decrease of the glass transition temperature of the polymer matrix with the molecular weight of the monomer. An increase of chain length between two adjacent crosslinking points leads to an enhanced molecular mobility and thus to lower values of the T_g (polymer matrix).

3.2. Infrared Spectroscopy

The kinetics of photopolymerization and the phase separation behavior of monomer/LC blends govern the architecture of the obtained polymer network.

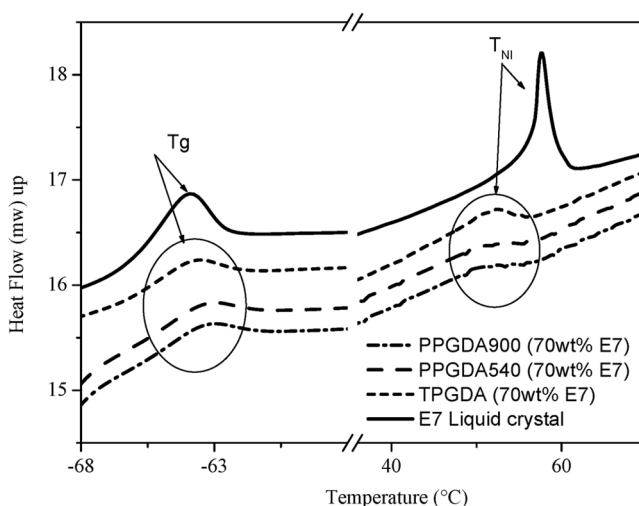


Figure 2. DSC curves of E7 and cured 30 wt% TPGDA/70 wt% E7, 30 wt% PPGDA540/70 wt% E7 and 30 wt% PPGDA900/70 wt% E7.

The three difunctional propyleneglycol based acrylic monomers used in this work give rise to chemically crosslinked polymer networks. In order to analyze the extent of formation of the polymer network, the relationship between the conversion of the monomers and the curing conditions was investigated. It is evident that high monomer conversions should be reached to minimize undesired effects of untreated monomers or dangling chains. FTIR spectroscopy was applied as versatile method to investigate the extent of curing via carbon-carbon double bond conversion.

Several absorption bands are available to monitor the polymerization/cross-linking processes and to evaluate the conversion of the acrylic double bonds of the monomers TPGDA, PPGDA540 and PPGDA900. One of the most characteristic absorption bands which is quite often used in IR-analysis of acrylates is the one corresponding to the $-\text{CH}=\text{CH}-$ deformation vibration at 810 cm^{-1} . Unfortunately, the LC E7 exhibits a strong absorption band near 810 cm^{-1} originating from the vibration of the phenyl group [15]. To circumvent the difficulty, coming from the overlap of these two bands, another band emerging at 1638 cm^{-1} is used for the analysis of the monomer/E7 blend. The calculation of the monomer conversion is made by considering the peak heights of the absorption band at 1638 cm^{-1} .

Table 1. Characteristic temperatures of E7 and cured 30 wt% TPGDA/70 wt% E7, 30 wt% PPGDA540/70 wt % E7, and 30 wt% PPGDA900/70 wt% E7

	E7	PPGD900 (70 wt%)	PPGDA540 (70 wt%)	TPGDA (70 wt%)
T_g (poly matrix) [°C]		-51	-41	-22
T_g (E7) [°C]	-65	-65	-66	-66
T_{NI} [°C]	58	52	53	54

The conversion ratio C is calculated using:

$$C (\%) = \frac{(A_{1638})_{(D=0)} - (A_{1638})_{(D)}}{(A_{1638})_{(D=0)}} \quad (3)$$

where $(A_{1638})_{D=0}$ is the height of the absorption band of the precursor system at 1638 cm^{-1} (i.e., radiation dose D is zero) and $(A_{1638})_D$ is the corresponding result for the system exposed to a dose D . Figure 3 represents the results of a FTIR spectroscopic analysis of three different systems based on 30 wt-% monomer and 70 wt-% E7. This figure shows the evolution of the acrylic double-bond conversion as a function of UV light exposure time. The inset of this figure shows the same results based on the range between 0 and 400 s. It can be observed that increasing irradiation doses lead to an uptake of the monomer conversion. The TPGDA system shows slower polymerization kinetics leading to lower conversion values compared to the other monomer mixtures. The TPGDA polymer network exhibits the highest crosslinking density of all systems studied here, leading to a relatively high glass transition temperature ($T_g = -22^\circ\text{C}$, compared to $T_g = -41^\circ\text{C}$ for cured PPGDA540 and $T_g = -51^\circ\text{C}$ for cured PPGDA900, see Table 1), and thus to a reduced monomer mobility during polymerization. As a result, the TPGDA system shows lower conversion values compared to the other systems. The PPGDA540 system reveals a sharp increase of the conversion/exposure time curve, in particular between 0 and 60 s, showing faster polymerization kinetics compared with the TPGDA system. This can be explained by the enhanced mobility of the reacting species in relation with the strongly reduced T_g due to the greater distance between acrylic functions. Further increase of the molecular weight of monomer leads to reduced probability of chain propagation. As a consequence, Figure 3 shows intermediate kinetics of the PPGDA900 system compared to PPGDA 540 and TPGDA.

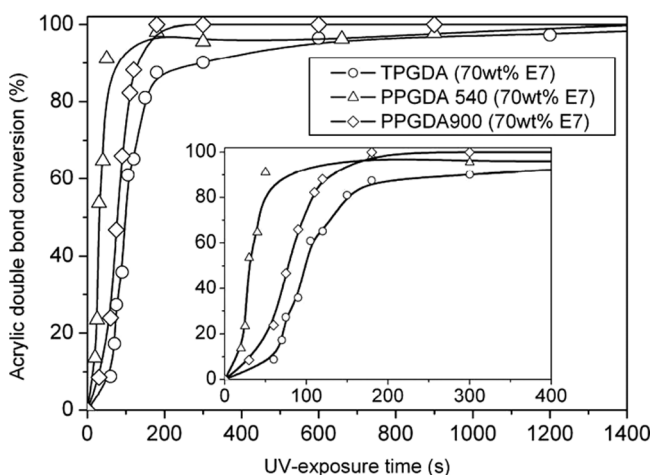


Figure 3. FTIR-analysis: conversion of acrylic double bonds of TPGDA, PPGDA540 and PPGDA900 prepared by UV curing using 70wt % E7 and 2wt% Darocur 1173 as photoinitiator.

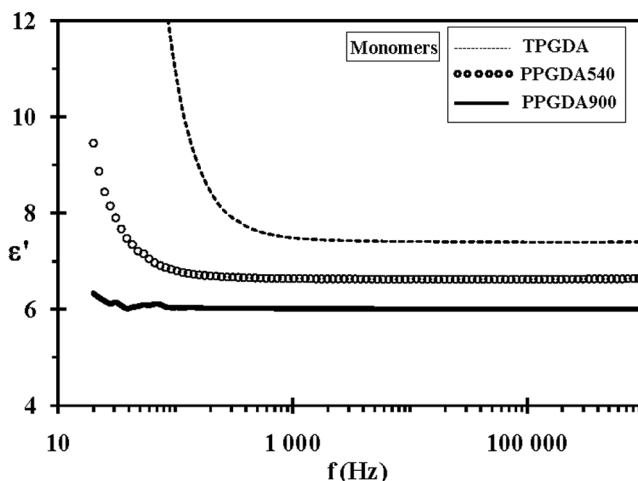


Figure 4. Real part of the dielectric spectra of the three monomers at room temperature.

These results show clearly that high conversions (>95%) were achieved in all cases considered here for exposure times higher than 400 s and that, therefore, one of the conditions necessary for good performance of PDLC films are fulfilled.

3.3. Dielectric Spectroscopy

Figures 4–6 show room temperature dielectric spectra (real part of permittivity $\epsilon'(f)$) corresponding to monomers, polymers, and polymer/LC systems (70 wt%E7), respectively. The conductivities of all materials are gathered in Table 2, and were calculated at low frequencies and from the imaginary part of the dielectric spectra ($\epsilon''(f)$): $\sigma = 2\pi f \epsilon'' \epsilon_0$.

In a wide frequency range ($f > 1$ kHz), the dielectric permittivities of the monomers are constant as shown in Figure 4. In the frequency range investigated here, the

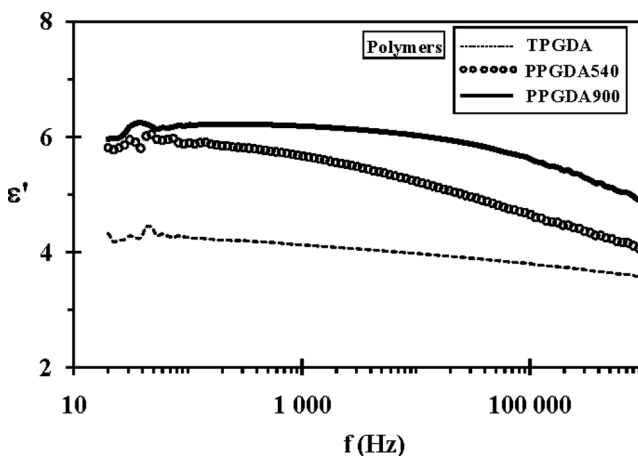


Figure 5. Real part of the dielectric spectra of the three polymers at room temperature.

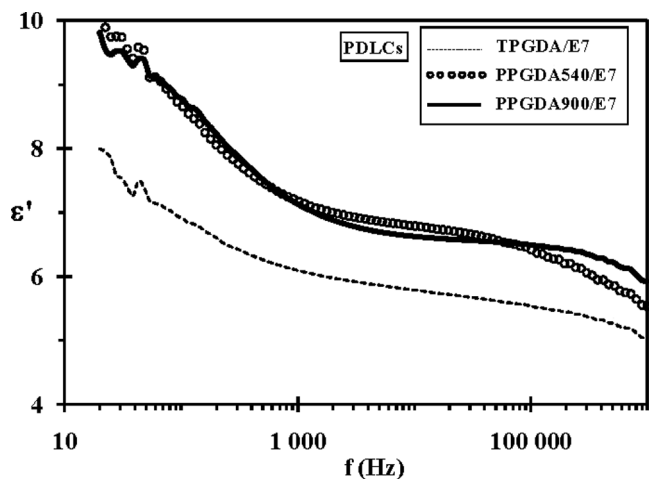


Figure 6. Real part of the dielectric spectra of the three polymer/LC systems (70 wt% E7) at room temperature.

three materials do not present the classical α dielectric relaxation process usually observed near the glass transition. In fact, the T_g of the monomers are very low compared to the room temperature (T_g TPGDA = -85°C ; T_g PPGDA540 = -74°C , T_g PPGDA900 = -70°C). At low frequencies ($f < 100$ Hz), the dielectric permittivity for the different materials increases when the frequency decreases. This effect, due to the accumulation of ionic charges near electrodes, is more pronounced on the TPGDA and the PPGDA540 monomers. This is in good agreement with the evolution of the ionic conductivity, which is higher for these two systems compared to PPGDA900 (Table 2). When the molecular weight of the monomer increases, the dielectric permittivity decreases ($\epsilon' = 7.2$ for TPGDA, $\epsilon' = 6.6$ for PPGDA540, $\epsilon' = 6.0$ for PPGDA900). Let us notice that the dipolar moment of the monomer molecules is mainly linked to that of the carbon-oxygen double bonds (C=O). The higher permittivity of the TPGDA monomer can be explained by its lower molecular length, which results in a higher volume density of C=O groups and thus a higher dipole moment.

The polymerization of TPGDA leads to a decrease of static permittivity ($\epsilon' = 4.2$), compared to that of the monomer ($\epsilon' = 7.2$), as shown in Figure 5. This difference decreases when the molecular length increases and was not observed for PPGDA900. This effect can be explained by the influence of the polymer network density. In fact, in the case of the TPGDA monomer, the chain length between

Table 2. Conductivities of monomers, polymers and PDLCS (70 wt% E7) ($\times 10^{-8}(\Omega \cdot \text{m})^{-1}$)

	Monomers	Polymers	PDLCS
TPGDA	160	<0.1	4.6
PPGDA540	27	<0.1	8.9
PPGDA900	9.3	~ 0.1	12.9

two adjacent crosslinking points is relatively low and the mobility of molecular chains and the dipolar response are affected by the polymer network. In the case of the PPGDA900, the polymer network exhibits a lower density and the dipolar response is similar to the one of monomer. This effect can be correlated to the ionic conductivity, which is linked to the ionic mobility. The dielectric relaxation process observed on polymers at high frequencies (100 kHz) is probably linked to a classical α process.

At low frequencies, the three PDLC systems present permittivities higher than those obtained for the pure polymers (Fig. 6). This can be explained by the contribution of the LC, which seems to present a predominant homeotropic orientation. In fact, the LC presents higher permittivity ($\epsilon'_{\parallel} = 19$) compared with that obtained in planar orientation ($\epsilon'_{\perp} = 5$). Let us notice that the TPGDA/E7 system presents the lowest permittivity. This can be explained by the lower permittivity value of the TPGDA polymer and/or by the polymer density effect. The mobility of the LC molecules and the dielectric response can be affected by the dense polymer network of TPGDA. The relaxation process observed at low frequencies for the three polymer/LC systems is probably correlated to the well known Maxwell-Wagner process (interfacial polarization). The relaxation process with frequency about 1 MHz corresponds to the LC dielectric process linked to the rotation around the short axis.

4. Conclusions

Spectroscopical, thermophysical and dielectrical response functions of UV-cured PPGDA/E7 films were investigated experimentally as function of the chain length of the monomer. The conversion of double bonds of the acrylate monomers was monitored by FTIR spectroscopy in terms of the radiation dose. The PPGDA 540/E7 blend shows the highest reactivity compared to the other systems. An upper limit of the double bond conversion was reached near 95–98%. A detailed analysis conducted by DSC measurements revealed decreasing polymer glass transition temperatures and decreasing nematic-isotropic transition temperatures of polymer/LC systems with increasing monomer chain length.

The dielectric permittivity increases in the order PPGDA900 – PPGDA540 – TPGDA which can be explained by the higher dipole moment of TPGDA caused by an enhanced volume density of carbonyl groups. Polymer/LC systems show relaxation processes at low frequencies which can probably be explained by the Maxwell-Wagner process. The presence of crosslinks in the polymer networks leads to reduced chain mobility and thus to a decrease of the static permittivity.

References

- [1] Mucha, M. (2003). *Prog. Polym. Sci.*, 28, 837.
- [2] Lampert, C. M. (2004). *Mater. Today*, 7, 28.
- [3] (1994). *Merck Liquid Crystals*, Licrilite Brochure.
- [4] Tarry, H. A. (1979). *The Refractive Indices of Cyanobiphenyl Liquid Crystals*, Merck Ltd., Merck House, Poole, Great Britain, 63.
- [5] Heavin, S. D., & Fung, B. M. (1991). *SPIE*, 1455, 13.
- [6] Roussel, F., Maschke, U., Coqueret, X., & Buisine, J.-M. (1998). *C. R. Acad. Sci.*, Paris, 449.
- [7] Roussel, F., Maschke, U., Coqueret, X., & Buisine, J.-M. (1998). *Liq. Cryst.*, 24, 555.

- [8] Russel, G. M., Paterson, B. J. A., & Imrie, C. T. (1995). *Chem. Mater.*, 7, 2185.
- [9] Nwabunma, D., Kim, K. J., Lin, Y., Chien, L. C., & Kyu, T. (1998). *Macromolecules*, 31, 6806.
- [10] Smith, G. W. (1994). *Mol. Cryst. Liq. Cryst.*, 241, 77.
- [11] Challa, S. R., Wang, S.-Q., & Koenig, J. L. (1995). *J. Therm. Anal.*, 45, 1297.
- [12] Roussel, F., Buisine, J.-M., Maschke, U., & Coqueret, X. (1997). *Mol. Cryst. Liq. Cryst.*, 299, 321.
- [13] Smith, G. W. (1991). *Mol. Cryst. Liq. Cryst.*, 196, 89.
- [14] Douali, R., Legrand, C., Faye, V., & Nguyen, H. T. (1999). *Mol. Cryst. Liq. Cryst.*, 328, 209.
- [15] Bentley, W. G., & Koenig, J. L. (1997). *Appl. Spectr.*, 51, 1453.